

Global evaluation of CMIP5 Earth System Models in simulating Leaf Area Index using remote sensing products

**Jiafu Mao^{1,*}, Forrest M. Hoffman², Jitendra Kumar¹, Xiaoying Shi¹,
Shishi Liu¹, Daniel M. Ricciuto¹, Peter E. Thornton¹, Hua Yuan³,
Yongjiu Dai³, Ranga B. Myneni⁴ and Zaichun Zhu⁴,**

¹Climate Change Science Institute/Environmental Sciences Division, Oak Ridge National Laboratory, Oak Ridge, Tennessee, USA

²Climate Change Science Institute/Computer Science and Mathematics Division, Oak Ridge National Laboratory, Oak Ridge, Tennessee, USA

³School of Geography, Beijing Normal University, Beijing 100875, China

⁴Department of Earth and Environment, Boston University, 675 Commonwealth Avenue, Boston, MA 02215, USA

**E-Mail: maoj@ornl.gov; Tel.: +1-865-576-7815; Fax: +1-865-574-9501.*

Modeling uncertainties

- *Initial conditions*
- *Internal processes*
- *Parameters*
- *Natural and human external forcings*

Global simulations and evaluations (LSM for example)

- *Test the model beyond the single-site calibration*
- *Performance of the model against large-scale “observations”, in particular the well-calibrated remote sensing data sets in recent decades*
- *Inform the model improvement and new measurements for next steps*
- *Improve understanding of ecosystem structure, function and climate-carbon cycle feedbacks at relevant spatial-temporal scales*

LAI related work at ORNL

- *Attribution studies of annual LAI change: Community Land Model (CLM) in CESM, Changing CO₂, Anthropogenic airborne nitrogen deposition and Dynamic LULCC (1982-2010) (Mao et al., 2013)*
- *Assessing the accuracy of prognostic LAI in fully-coupled Earth System Models (ESMs) from the Coupled Model Intercomparison Project Phase 5 (CMIP5)*

Global Latitudinal-Asymmetric Vegetation Growth Trends and Their Driving Mechanisms: 1982-2009

Contact: Jiafu Mao, 865-576-7815, maoj@ornl.gov

Funding: DOE Office of Science, Biological and Environmental Research

Citation: Mao J, Shi X, Thornton PE, Hoffman FM, Zhu Z, Myneni RB. Global Latitudinal-Asymmetric Vegetation Growth Trends and Their Driving Mechanisms: 1982–2009. *Remote Sensing*. 2013; 5(3): 1484-1497.

Objective

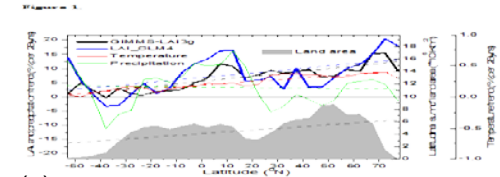
Application of CLM4 and a latest satellite-derived LAI to investigate annual trend changes and controlling factors of global vegetation growth from the period 1982 to 2009.

New Science

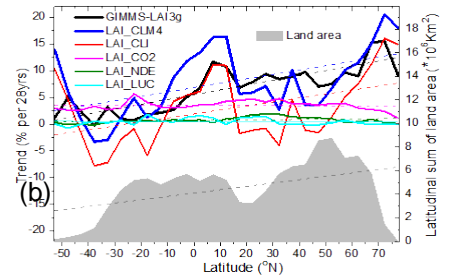
- Over the 28-year period, both the remote-sensing estimate and CLM4 simulation show a significant increasing trend in annual vegetation growth.
- Latitudinal asymmetry appeared in both products, with small increases in the Southern Hemisphere and larger increases at high latitudes in the Northern Hemisphere.
- The south-to-north asymmetric land surface warming was assessed to be the principal driver of this latitudinal asymmetry of LAI trend.
- Heterogeneous precipitation decreased this latitudinal LAI gradient, and considerably regulated the local LAI change.
- CO₂ fertilization during the last three decades was estimated to be the dominant cause for enhancement in global mean vegetation growth.
- Human induced land use/land cover change and nitrogen deposition produced slightly increasing global LAI and the regionally dependent impacts.

Significance

- Model-data analysis provides process attribution information not available from the observations alone.
- Simulated CLM4 LAI compares well with an independent satellite-based estimate in terms of annual trends and correlations with climate.
- These validation exercises provide new global-scale metrics for evaluation of model outputs and help prioritize improvements in model performance across different scales.

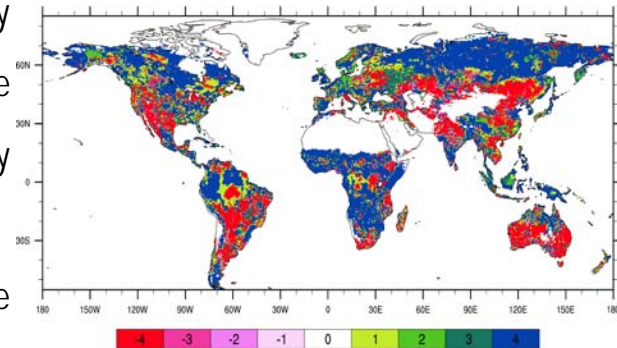


(a)



(b)

Latitudinal gradient of percentage change (%/28 yrs) in (a) GIMMS-LAI3g, LAI_CLM4, temperature and precipitation, and (b) simulated single-factor LAI for 1982–2009.



Simulated dominant driving factors for LAI trends between 1982 and 2009

-4 decrease due to Climates	-1 decrease due to CO2	2 increase due to N Dep
-3 decrease due to LULCC	0 no trend	3 increase due to LULCC
-2 decrease due to N Dep	1 increase due to CO2	4 increase due to Climates

Modeling uncertainties

- *Initial conditions*
- *Internal processes*
- *Parameters*
- *Natural and human external forcings*

Global simulations and evaluations (LSM for example)

- *Test the model beyond the single-site calibration*
- *Performance of the model against large-scale “observations”, in particular the well-calibrated remote sensing data sets in recent decades*
- *Inform the model improvement and new measurements for next steps*
- *Improve understanding of ecosystem structure, function and climate-carbon cycle feedbacks at relevant spatial-temporal scales*

LAI related work at ORNL

- *Attribution studies of annual LAI change: Community Land Model (CLM) in CESM, Changing CO₂, Anthropogenic airborne nitrogen deposition and Dynamic LULCC (1982-2010)*
- *Assessing the accuracy of prognostic LAI in fully-coupled Earth System Models (ESMs) from the Coupled Model Intercomparison Project Phase 5 (CMIP5)*

CMIP5 models

- *24 fully-coupled ESMs*
- *Using multi-realization mean for each model group*
- *Diagnostic CO₂ and prognostic LAI for the period of overlap (2000 and 2009)*
- *RCP8.5 for year 2006 to 2009*

Global remote sensing LAI products

- *MODIS Collection 5 LAI data*
- *GIMMS LAI3g (based on the MODIS LAI, AVHRR GIMMS NDVI3g and Artificial Neural Network model) (Zhu et al., 2013)*
- *BNU LAI (improved MODIS LAI) (Yuan et al., 2011)*

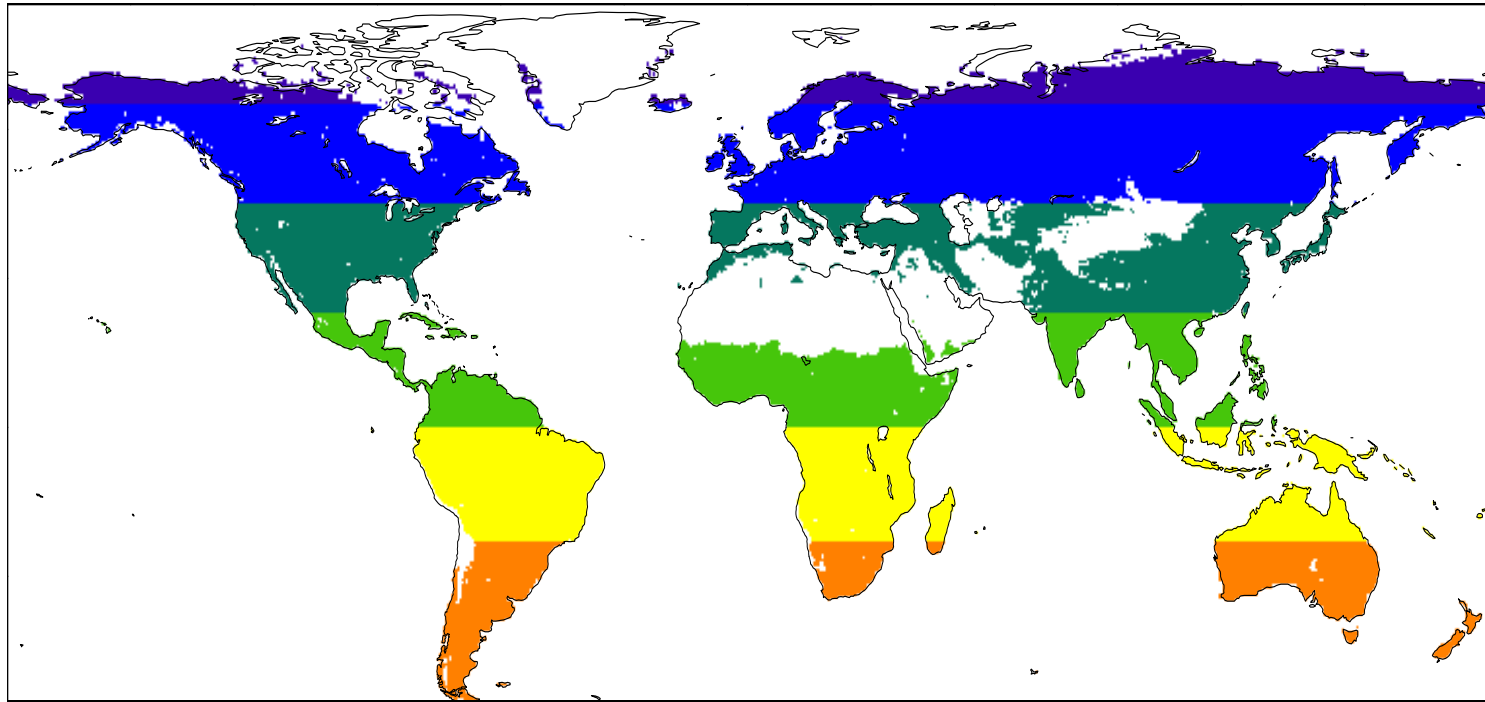
Methods

- *Gap-filling of satellite LAI*
- *Remapping to global half-degree*
- *Global, each hemisphere and six latitudinal bands*
- *Seasonal cycle, mean, and trend et al.*

Introduction | Data sets and Methods | Findings | Summary

Model	Modeling Center (or Group)	Atmosphere	Component Models and Resolutions		
			Land	Ocean	Sea Ice
BCC-CSM1.1 (Wu et al., submitted)	Beijing Climate Center, China Meteorological Administration, CHINA	AGCM2.1 ($2.875^\circ \times 2.875^\circ$, L26)	AVIM1.0 ($2.875^\circ \times 2.875^\circ$)	MOM4_L40 ($1^\circ \times (1-\frac{1}{3})^\circ$, L40)	SIS ($1^\circ \times (1-\frac{1}{3})^\circ$)
BCC-CSM1.1(m) (Wu et al., submitted)	Beijing Climate Center, China Meteorological Administration, CHINA	AGCM2.1 ($2.875^\circ \times 2.875^\circ$, L26)	AVIM1.0 ($2.875^\circ \times 2.875^\circ$)	MOM4_L40 ($1^\circ \times (1-\frac{1}{3})^\circ$, L40)	SIS ($1^\circ \times (1-\frac{1}{3})^\circ$)
BNU-ESM [†] (Dai et al., 2003, 2004)	Beijing Normal University, CHINA	CAM3.5 ($2.875^\circ \times 2.875^\circ$, L26)	CoLM3 & BNUDGVM (C/N) ($2.875^\circ \times 2.875^\circ$, L10)	MOM4p1 & IBGC ($1^\circ \times (1-\frac{1}{3})^\circ$, L50)	CICE4.1 ($1^\circ \times (1-\frac{1}{3})^\circ$)
CanESM2 [‡] (Arora et al., 2011)	Canadian Centre for Climate Modelling and Analysis, CANADA	CanAM4 ($2.81^\circ \times 2.81^\circ$, L35)	CLASS2.7 & CTEM1 ($2.81^\circ \times 2.81^\circ$)	CanOM4 & CMOC1.2 ($1.5^\circ \times 1^\circ$, L40)	CanSIM1 ($2.81^\circ \times 2.81^\circ$)
CESM1-BGC (Hurrell et al., in press)	Community Earth System Model Contributors, NSF-DOE-NCAR, USA	CAM4 ($0.9^\circ \times 1.25^\circ$, L30)	CLM4 ($0.9^\circ \times 1.25^\circ$)	POP2 & NPZD ($1^\circ \times (1-\frac{1}{3})^\circ$, L60)	CICE4 ($1^\circ \times (1-\frac{1}{3})^\circ$)
FGOALS-s2 ^a (Bao et al., in press)	LASG, Institute of Atmospheric Physics, CAS, CHINA	SAMIL2.4.7 ($1.67^\circ \times 2.81^\circ$, L26)	CLM3 & VEGAS2.0 ($1.67^\circ \times 2.81^\circ$)	LICOM2.0 ($1^\circ \times (1-\frac{1}{2})^\circ$, L30)	CSIM5 ($1^\circ \times (1-\frac{1}{2})^\circ$)
GFDL-ESM2g, GFDL-ESM2m ^b (Dunne et al., 2012, 2013)	NOAA Geophysical Fluid Dynamics Laboratory, USA	AM2 ($2^\circ \times 2.5^\circ$, L24)	LM3 ($2^\circ \times 2.5^\circ$)	MOM4 ($1^\circ \times (1-\frac{1}{3})^\circ$, L50)	SIS ($1^\circ \times (1-\frac{1}{3})^\circ$)
HadGEM2-ES ^c (Collins et al., 2011; Jones et al., 2011)	Met Office Hadley Centre, UNITED KINGDOM	HadGAM2 & UKCA ($1.25^\circ \times 1.875^\circ$, L38)	MOSES2 & TRIFFID ($1.25^\circ \times 1.875^\circ$)	HadGOM2 & diat-HadOCC ($1^\circ \times (1-\frac{1}{3})^\circ$, L40)	HadGOM2 ($1^\circ \times (1-\frac{1}{3})^\circ$)
INM-CM4 ^{†‡} (Volodin et al., 2010)	Institute for Numerical Mathematics, RUSSIA	($2^\circ \times 1.5^\circ$, L21)	($2^\circ \times 1.5^\circ$)	($1^\circ \times 0.5^\circ$, L40)	($1^\circ \times 0.5^\circ$)
IPSL-CM5A-LR ^d (Dufresne et al., 2013)	Institut Pierre-Simon Laplace, FRANCE	LMDZ4 ($3.75^\circ \times 1.9^\circ$, L39)	ORCHIDEE ($3.75^\circ \times 1.9^\circ$)	ORCA2 & PISCES ($2^\circ \times (2-\frac{1}{2})^\circ$, L31)	LIM2 ($2^\circ \times (2-\frac{1}{2})^\circ$)
MIROC-ESM (Watanabe et al., 2011; Oschlies, 2001)	JAMSTEC, University of Tokyo, and NIES, JAPAN	MIROC-AGCM & SPRINTARS ($2.875^\circ \times 2.875^\circ$, L80)	MATSIRO & SEIB-DGVM ($2.875^\circ \times 2.875^\circ$, L6)	COCO3.4 & NPZD ($1.5^\circ \times 1^\circ$, L44)	COCO3.4 ($1.5^\circ \times 1^\circ$)
MPI-ESM-LR ^e (Maier-Reimer et al., 2005)	Max Planck Institute for Meteorology, GERMANY	ECHAM6 ($2.81^\circ \times 2.81^\circ$, L47)	JSBACH ($2.81^\circ \times 2.81^\circ$)	MPIOM & HAMOCC ($1.5^\circ \times 1.5^\circ$, L40)	MPIOM ($1.5^\circ \times 1.5^\circ$)
MRI-ESM1 (Yukimoto et al., 2011)	Meteorological Research Institute, JAPAN	GSMUV ($0.75^\circ \times 0.75^\circ$, L48)	HAL & MRI-LCCM2 ($0.75^\circ \times 0.75^\circ$)	MRI.COM3 ($1^\circ \times 0.5^\circ$, L51)	MRI.COM3 ($1^\circ \times 0.5^\circ$)
NorESM1-ME (Bentsen et al., 2012)	Norwegian Climate Centre, NORWAY	CAM-Oslo ($1.9^\circ \times 2.5^\circ$, L26)	CLM4 ($1.9^\circ \times 2.5^\circ$)	BOM & HAMOCC ($1^\circ \times (1-\frac{1}{3})^\circ$, L53)	CICE4 ($1^\circ \times (1-\frac{1}{3})^\circ$)

Climate zones used for summary



6

1 Arctic

2 Boreal

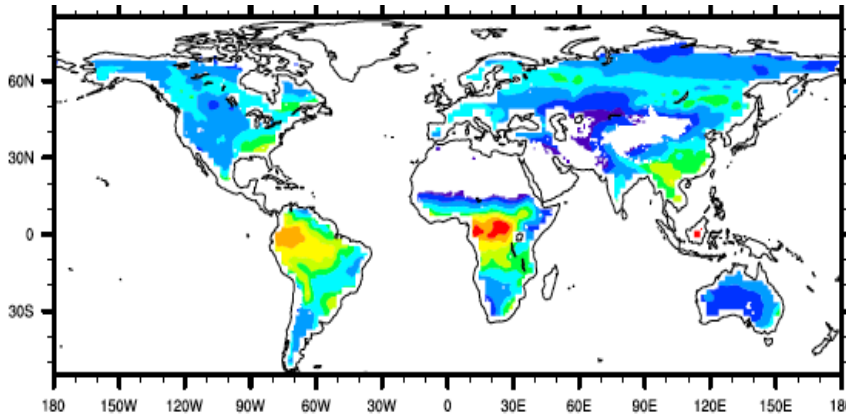
3 Northern Temperate

4 Northern Equatorial

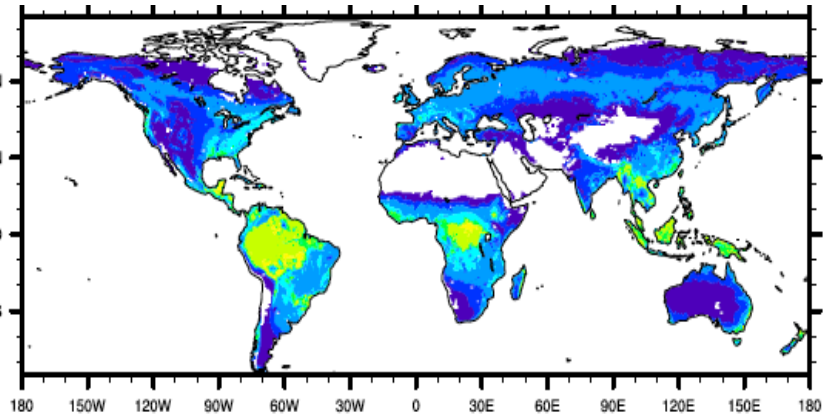
5 Southern Equatorial

6 Southern Temperate

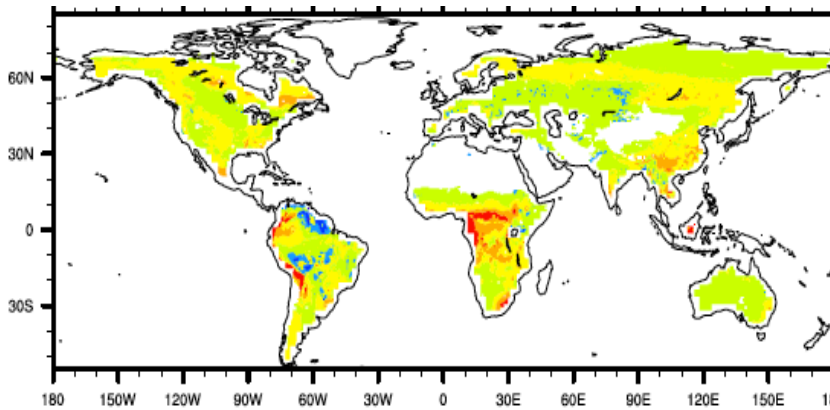
Model mean



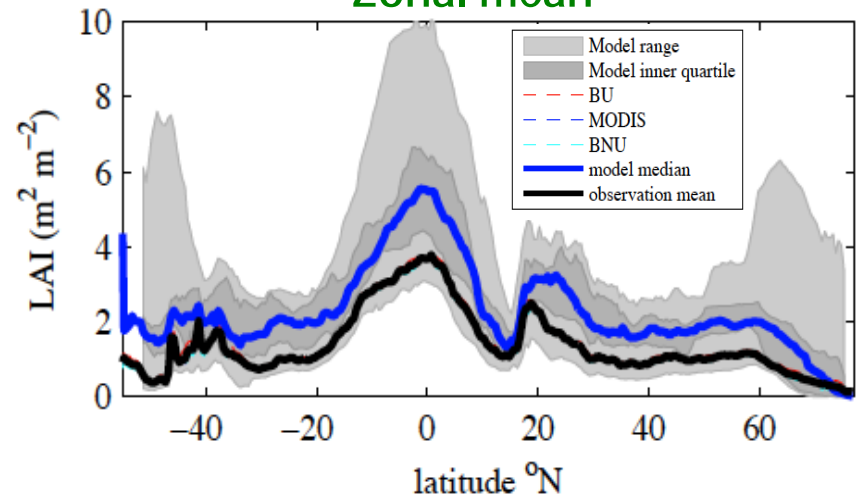
Obs. mean



Difference

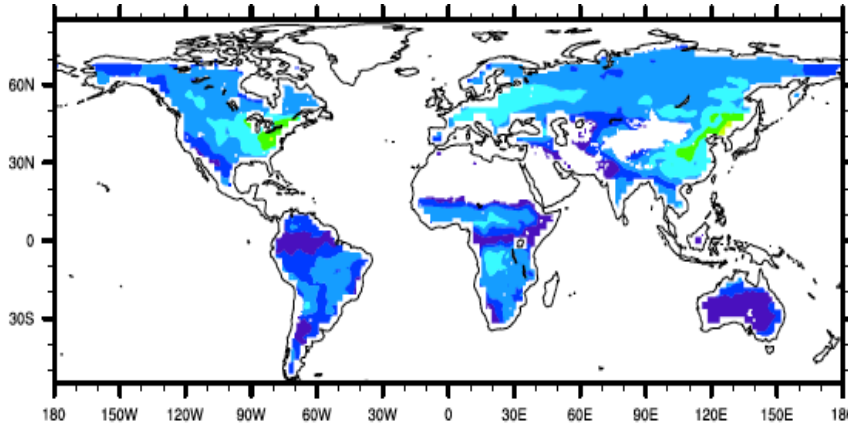


Zonal mean

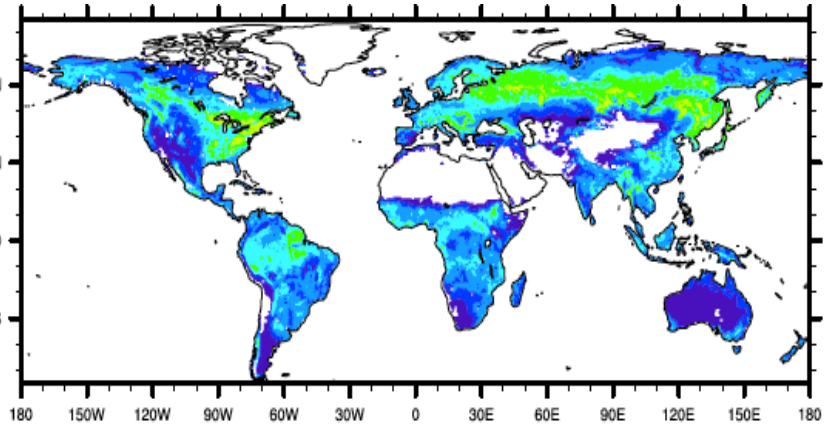


Annual mean LAI between 2000 and 2009

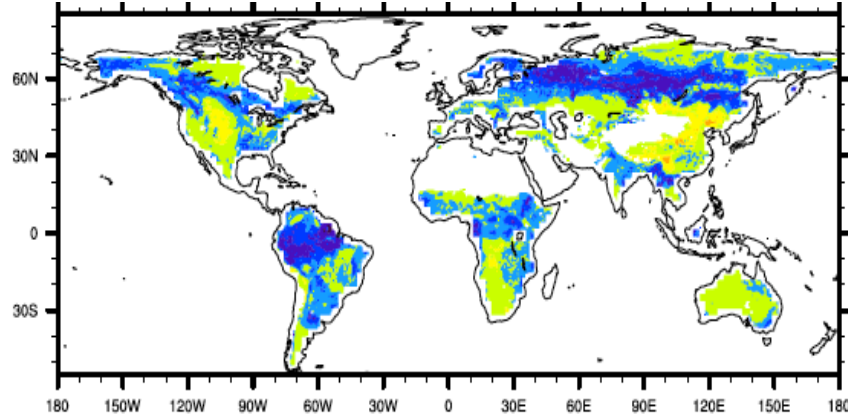
Model mean



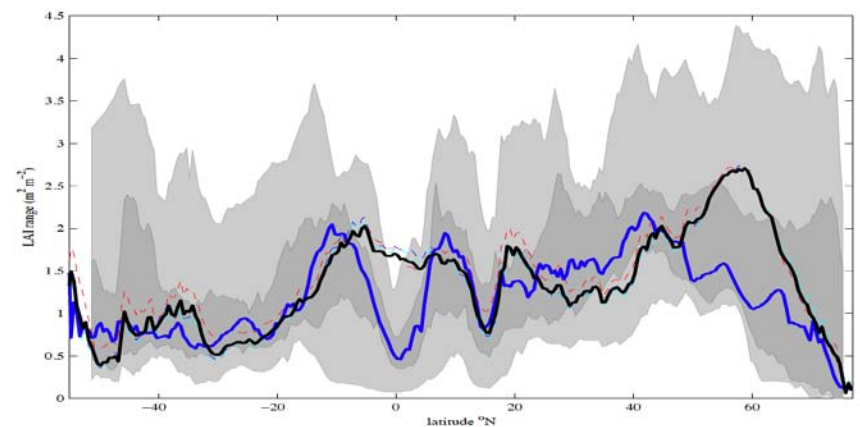
Obs. mean



Difference

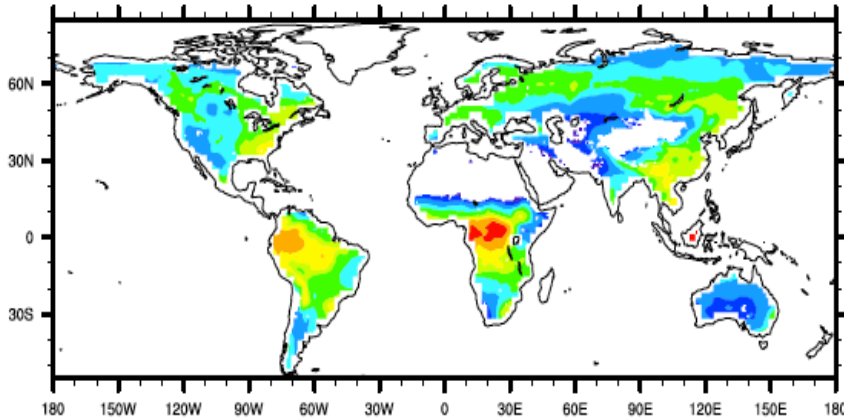


Zonal mean

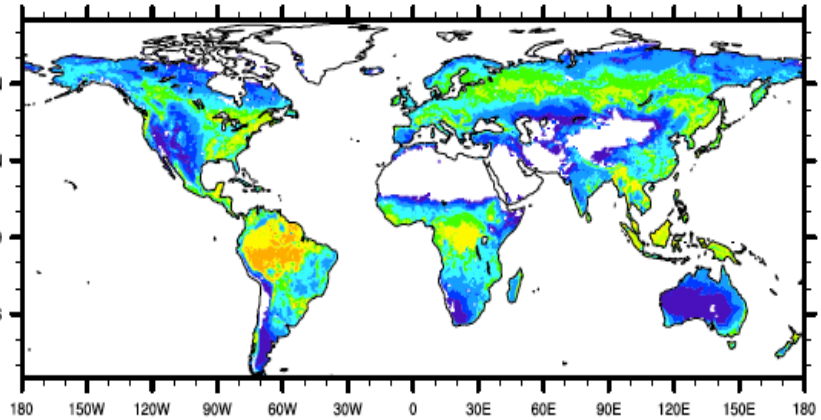


Mean LAI range between 2000 and 2009

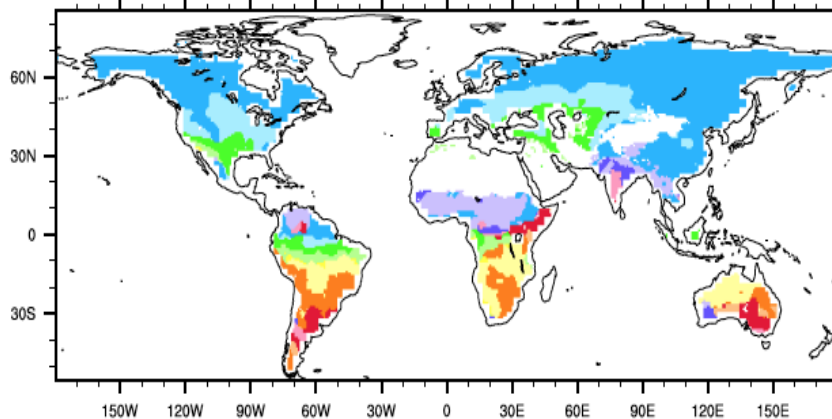
Model mean



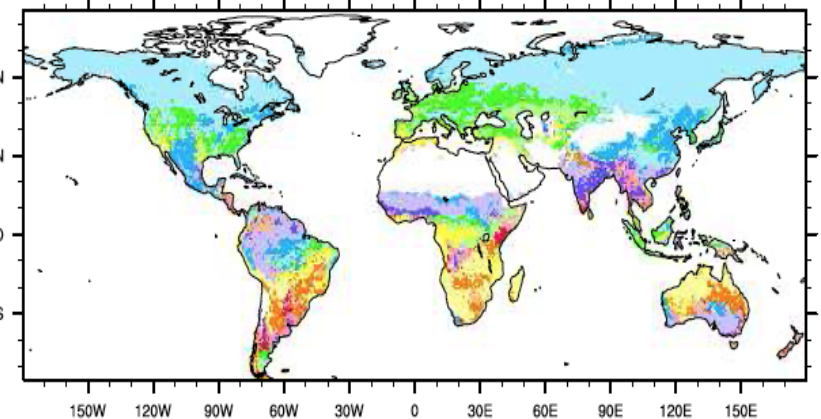
Obs. mean



Model mean

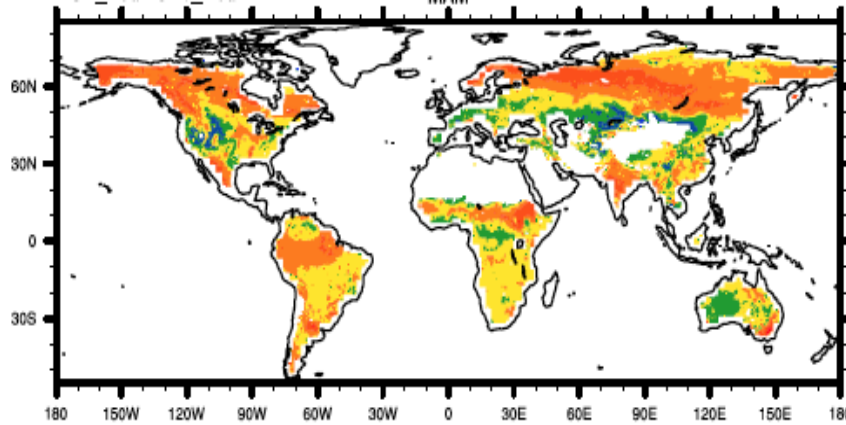


Obs. mean

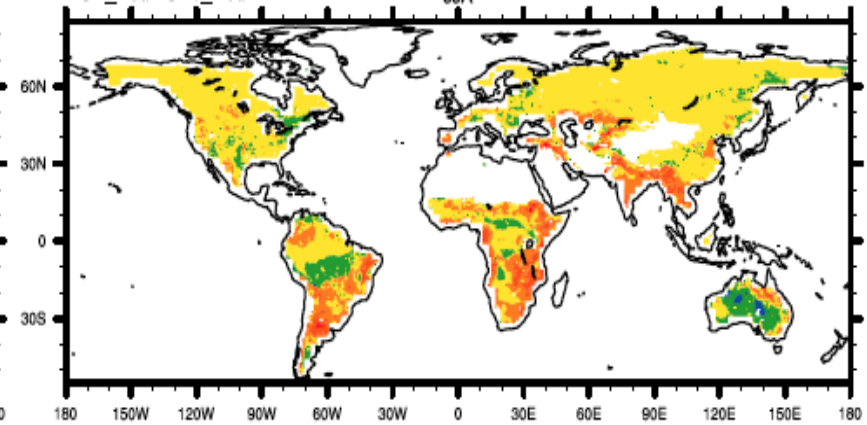


Maximum LAI and peak month

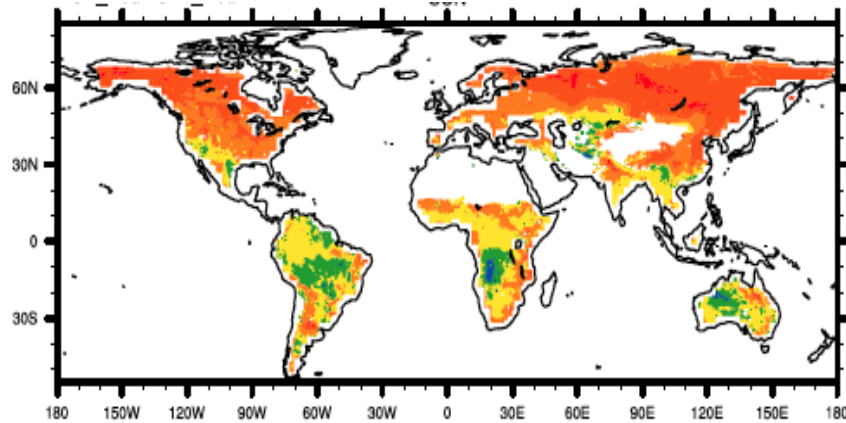
MAM



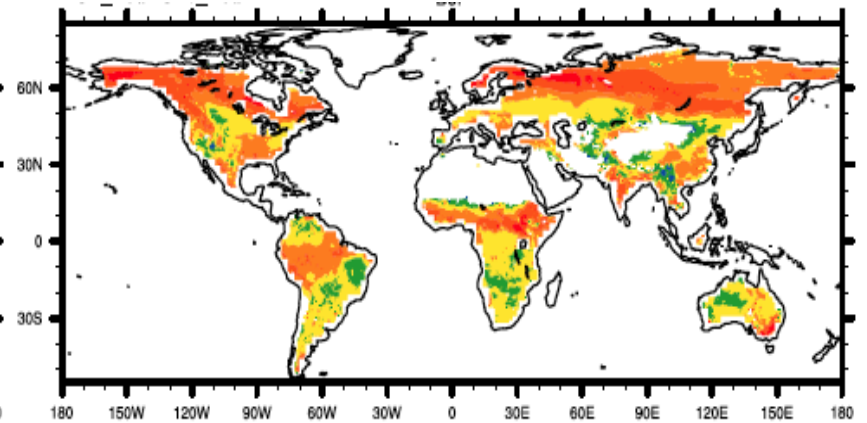
JJA



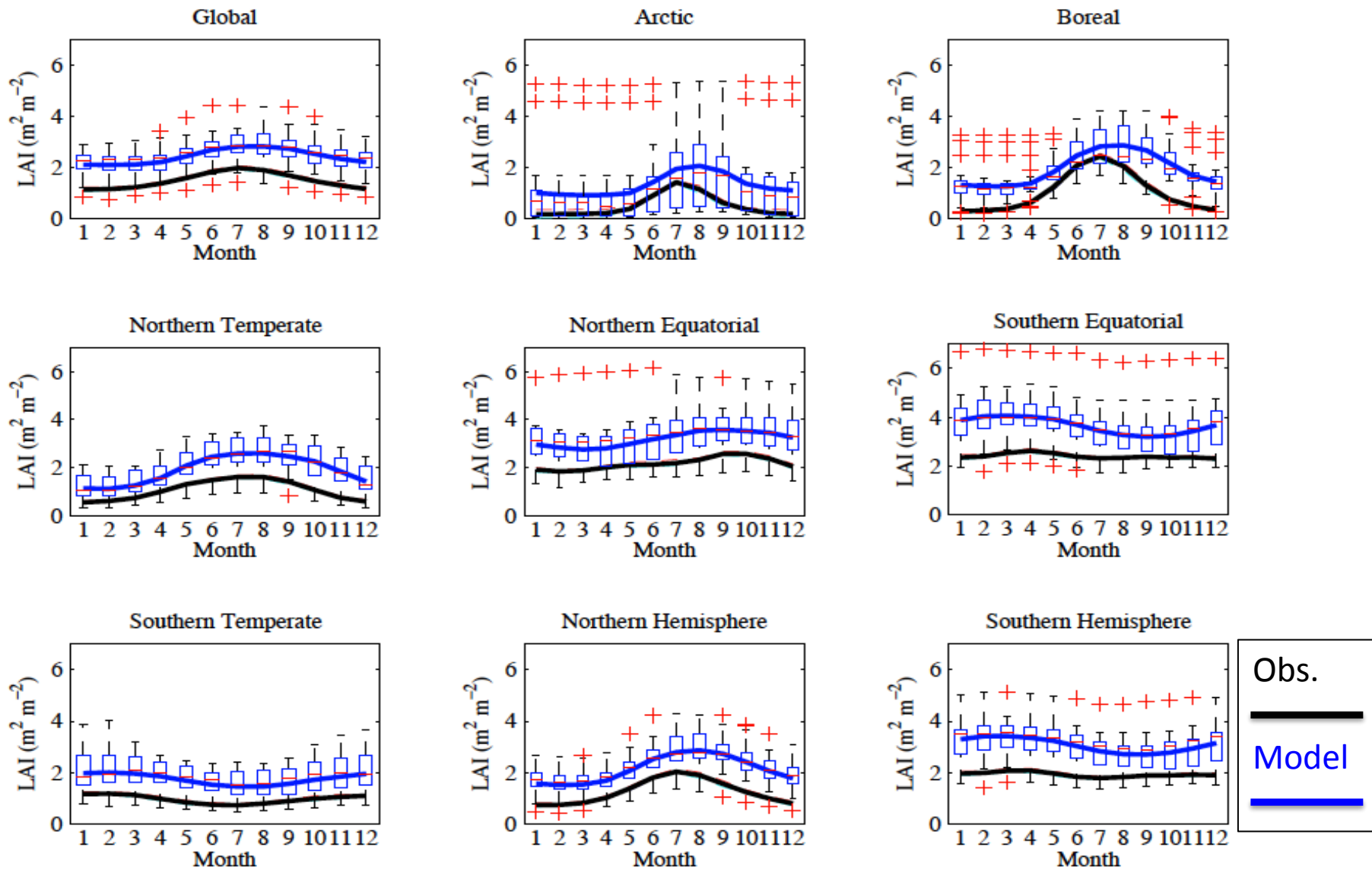
SON



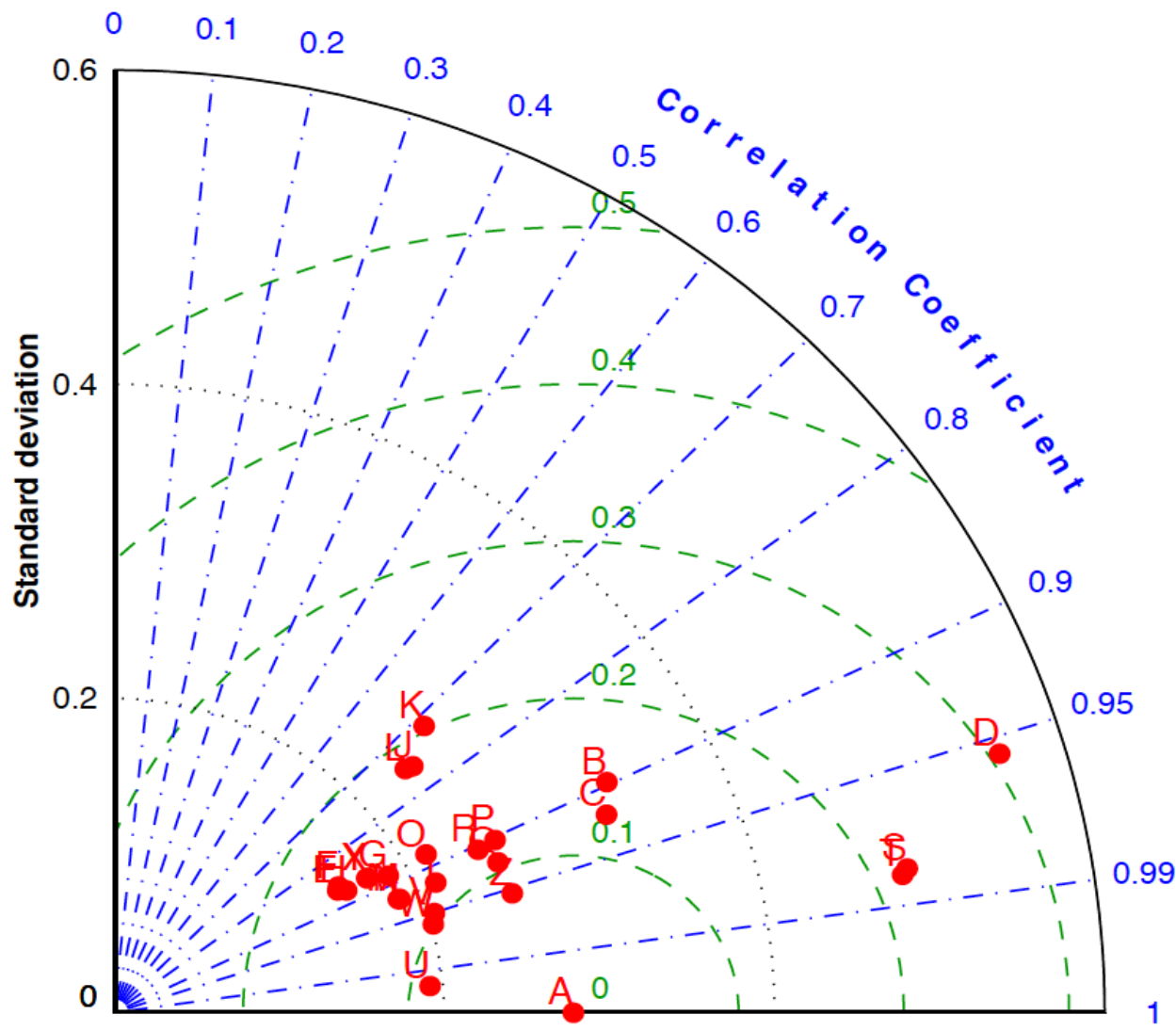
DJF



Normalized LAI difference for different season



LAI annual cycle over different zones



- A observed_ensemble mean
- B BCC-CSM1.1-M
- C BCC-CSM1.1
- D BNU-ESM
- E CCSM4
- F CESM1-BGC
- G CESM1-CAM5
- H CESM1-WACCM
- I CanESM2
- J GFDL-CM3
- K GFDL-ESM2G
- L GFDL-ESM2M
- M HadGEM2-CC
- N HadGEM2-ES
- O INM-CM4
- P IPSL-CM5A-LR
- Q IPSL-CM5A-MR
- R IPSL-CM5B-LR
- S MIROC-ESM-CHEM
- T MIROC-ESM
- U MIROC5
- V MPI-ESM-LR
- W MPI-ESM-MR
- X NorESM1-ME
- Y NorESM1-M
- Z model_ensemble_mean

Taylor plot of LAI annual cycle for each model

- ✧ Higher LAI absolute value, lower seasonality and longer growing season were generally identified
- ✧ Tropical and high latitudes have big uncertainties
- ✧ Extension of many existing CMIP5 evaluations with satellite products, and better understanding of the consistencies and discrepancies among different models
- ✧ New global-scale metrics for evaluation of model outputs and help prioritize improvements in model performance across different scales
- ✧ Annual trends, environmental correlations and implications for carbon and hydrology cycles

Thank you for attention!
Questions and comments?